

Journal of Materials Chemistry C

Materials for optical, magnetic and electronic devices

rsc.li/materials-c



Themed issue: Materials for thermally activated delayed fluorescence

ISSN 2050-7526

COMMUNICATION

Nobuo Kimizuka, Nobuhiro Yanai *et al.*
Heavy metal-free visible-to-UV photon upconversion with
over 20% efficiency sensitized by a ketocoumarin derivative



Cite this: *J. Mater. Chem. C*, 2022, 10, 4558

Received 16th November 2021,
Accepted 5th January 2022

DOI: 10.1039/d1tc05526g

rsc.li/materials-c

Heavy metal-free visible-to-UV photon upconversion with over 20% efficiency sensitized by a ketocoumarin derivative†

Masanori Uji,^a Naoyuki Harada,^a Nobuo Kimizuka,^a Masaki Saigo,^b Kiyoshi Miyata,^b Ken Onda^b and Nobuhiro Yanai^{a,c}

Efficient triplet–triplet annihilation-based photon upconversion (TTA-UC) from visible to UV light without using heavy metals is still a challenging task. Here we achieve a record-high TTA-UC efficiency of 20.3% among 100% maximum by employing a ketocoumarin derivative as a triplet sensitizer, which shows strong visible absorption, weak UV absorption, and efficient intersystem crossing.

With the necessity to expand the use of renewable energy, sunlight is one of the most powerful energy resources in our environment. Photon upconversion (UC) from visible light (vis, $\lambda > 400$ nm) to ultraviolet light (UV, $\lambda < 400$ nm) is attracting attention in applications such as photocatalytic fuel production and environmental cleanup. Triplet–triplet annihilation-based UC (TTA-UC) is particularly useful since it works at low excitation intensity.^{1–10} In the typical TTA-UC mechanism, the donor molecule is photo-excited to an S_1 state, followed by intersystem crossing (ISC) from S_1 to T_1 . Triplet energy transfer (TET) from donor to acceptor is followed by annihilation between two acceptor triplets and generation of an acceptor S_1 (Fig. 1).

Since the first report of vis-to-UV TTA-UC in 2006,¹¹ various donor–acceptor combinations have been reported, but the efficiency had remained low for a long time.^{11–27} Our group has achieved the highest TTA-UC efficiency η_{UC} of 20.5% (theoretical maximum: 100%) in 2020, which was twice as high as the previous record.²⁸ This is due to the use of an Ir-coumarin complex $\text{Ir}(\text{C6})_2(\text{acac})$ with strong absorption in the

visible region and weak absorption in the UV region as a donor, as well as the discovery of an acceptor 1,4-bis((triisopropylsilyl)ethynyl)naphthalene (TIPS-Nph) with high TTA and fluorescence efficiencies and a T_1 energy low enough to be sensitized by $\text{Ir}(\text{C6})_2(\text{acac})$. Subsequently, similar efficiencies have been reported by using semiconductor nanocrystals as donor and 2,5-diphenyloxazole (PPO) as acceptor.²⁹ However, these most efficient vis-to-UV TTA-UC systems use donors containing heavy metal ions such as Ir and Cd, which are not sustainable from the perspective of resource and environmental issues. Several examples of heavy metal-free vis-to-UV TTA-UC have been reported, but even the most efficient one showed a low TTA-UC efficiency of 8.2%.^{20–27} In addition, the threshold excitation intensity I_{th} is so high that it exceeds 1 W cm^{-2} in many cases. It is strongly desired to realize TTA-UC with both high efficiency and low I_{th} without using heavy metals.

Here, we show the highest η_{UC} of 20.3% as a heavy metal-free vis-to-UV TTA-UC, which is more than two times higher than

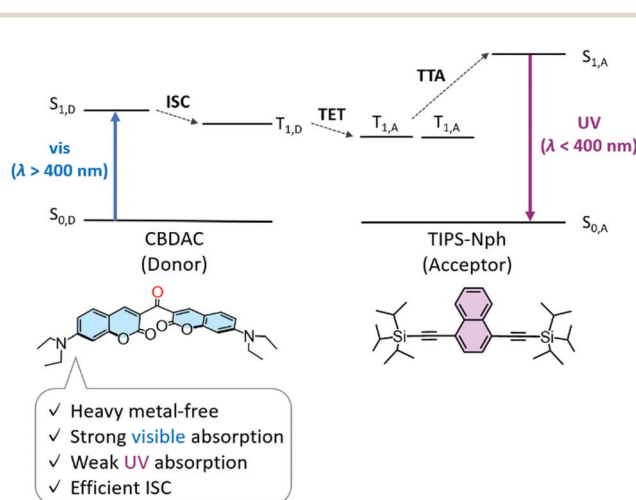


Fig. 1 Energy level diagram of vis-to-UV TTA-UC using a heavy metal-free donor CBDAC and an acceptor TIPS-Nph.

^a Department of Applied Chemistry, Graduate School of Engineering, Center for Molecular Systems (CMS), Kyushu University, 744 Moto-oka, Nishi-ku, Fukuoka 819-0395, Japan. E-mail: yanai@mail.cstm.kyushu-u.ac.jp, n-kimi@mail.cstm.kyushu-u.ac.jp

^b Department of Chemistry, Kyushu University, 744 Moto-oka, Nishi-ku, Fukuoka 819-0395, Japan

^c PRESTO, JST, Honcho 4-1-8, Kawaguchi, Saitama 332-0012, Japan

† Electronic supplementary information (ESI) available: Experimental details, DFT calculations, absolute and relative UC efficiencies, UC emission and transient absorption decays, parameters related to UC efficiency, fluorescence spectra, and threshold excitation intensity. See DOI: 10.1039/d1tc05526g

the previous record. Since the excellent absorption properties of $\text{Ir}(\text{C6})_2(\text{acac})$ originate from the ligand coumarin derivative, we searched for a coumarin derivative that does not contain heavy metals and shows efficient ISC, and found 3,3'-carbonylbis(7-diethylaminocoumarin) (CBDAC, Fig. 1), which has been used for TTA-UC in the visible range but not for vis-to-UV TTA-UC.³⁰

It is widely known that chromophores with carbonyl groups such as benzophenone exhibit high ISC efficiency Φ_{ISC} even without heavy metals due to the large spin-orbit coupling (SOC) caused by the distinct change in orbital symmetry during the transition from the $n-\pi^*/\pi-\pi^*$ singlet state to the $\pi-\pi^*/n-\pi^*$ triplet state.^{20,30–37} Ketocoumarin derivatives have also been used as heavy metal-free triplet sensitizers with such characteristics.^{30–33} Among the reported ketocoumarin derivatives, we focused on CBDAC because of its large absorption coefficient in the visible region over $70\,000\text{ M}^{-1}\text{ cm}^{-1}$ and weak absorption in the UV region (Fig. S1, ESI†),^{30–33} and it has been reported to have a high Φ_{ISC} of 92% in benzene.³¹

To understand the high Φ_{ISC} of CBDAC, we performed density functional theory (DFT) calculations. After structural optimization in the ground state, we calculated absorption bands and observed an absorption peak at 447 nm (2.77 eV), which is in good agreement with the experimental result (446 nm, Fig. 2). The energy level of S_1 was lower than that of T_3 (3.03 eV) and higher than that of T_1 and T_2 (2.20 eV) (Fig. S2a, ESI†). Focusing on the molecular orbitals involved in the ISC from S_1 to T_1 or T_2 , we found the orbital changes from HOMO to HOMO–1 and from LUMO to LUMO+1, both of which involve the significant contribution of the carbonyl groups (Fig. S2b and c, ESI†). It is suggested that the large orbital symmetry changes involving the carbonyl groups lead to the highly efficient ISC.

Importantly, CBDAC exhibits a strong and sharp absorption band, which is beneficial to suppress the absorption in the UV region. It was confirmed from the absorption and photoluminescence spectra that CBDAC and TIPS-Nph are a combination with suitable energy levels for vis-to-UV TTA-UC (Fig. 2). A toluene solution of CBDAC (100 μM) showed an absorption

peak at 446 nm (2.78 eV) and a fluorescence peak at 481 nm (2.58 eV). The high Φ_{ISC} of CBDAC was also supported by its low fluorescence quantum yield Φ_{FL} of 1.6% in toluene ($\lambda_{\text{ex}} = 445\text{ nm}$). A toluene solution of TIPS-Nph (100 μM) showed an absorption peak at 350 nm (3.54 eV) and a fluorescence peak at 373 nm (3.32 eV), with a Φ_{FL} of 74.8% ($\lambda_{\text{ex}} = 320\text{ nm}$). The T_1 energy levels of CBDAC and TIPS-Nph were estimated from phosphorescence measurements at 77 K in toluene (Fig. 2). CBDAC and TIPS-Nph showed 0–0 emission peaks at 557 nm (2.23 eV) and 586 nm (2.12 eV),³⁸ respectively. Good agreement was found between the DFT calculation and experimental results for the T_1 energy level of CBDAC. It is confirmed that the triplet energy level of CBDAC is high enough to sensitize TIPS-Nph.

As expected from the energy level matching, an upconverted UV emission was observed by exciting a deaerated toluene solution of CBDAC and TIPS-Nph with a 445 nm laser (Fig. 3a, [CBDAC] = 100 μM , [TIPS-Nph] = 10 mM). This mixed solution showed a remarkably high TTA-UC efficiency η_{UC} of 20.3%, which was determined by the relative method (Fig. 3b, maximum $\eta_{\text{UC}} = 100\%$,³⁹ see the ESI† for details). Note that we did not include corrections of inner-filter effect or reabsorption in the relative method in order to evaluate the performance as an UC material. We confirmed the reliability of this high η_{UC} value by observing a similar value of 21.5% with the absolute method using an integrating sphere (Fig. S3, see the ESI† for details).^{40,41} The obtained η_{UC} was more than twice larger than the previous record of 8.2% for the heavy metal-free vis-to-UV TTA-UC.²⁶ The triplet-mediated UC mechanism was confirmed by a millisecond-scale decay of the UC emission (Fig. S4, ESI†). Moreover, the UC emission intensity did not change even after one hour of continuous laser irradiation, demonstrating the high photostability of the current system (Fig. S5, ESI†).

The present heavy metal-free TTA-UC system was compared with the previous most efficient vis-to-UV TTA-UC system, $\text{Ir}(\text{C6})_2(\text{acac})$ and TIPS-Nph.²⁸ Since the solvents used in the previous and current reports are different, we used toluene as the solvent in this report for comparison. The mixed solution of

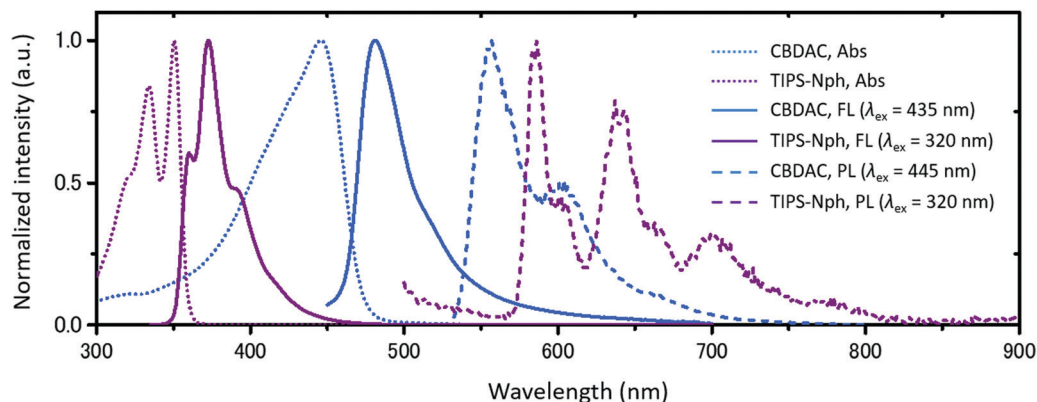


Fig. 2 Normalized absorption (dotted lines) and fluorescence (solid lines) spectra of CBDAC (100 μM , blue lines) and TIPS-Nph (100 μM , purple lines) at room temperature in deaerated toluene, and normalized phosphorescence spectra (dashed lines) of CBDAC (100 μM , blue) and TIPS-Nph (10 mM, purple) in toluene at 77 K.

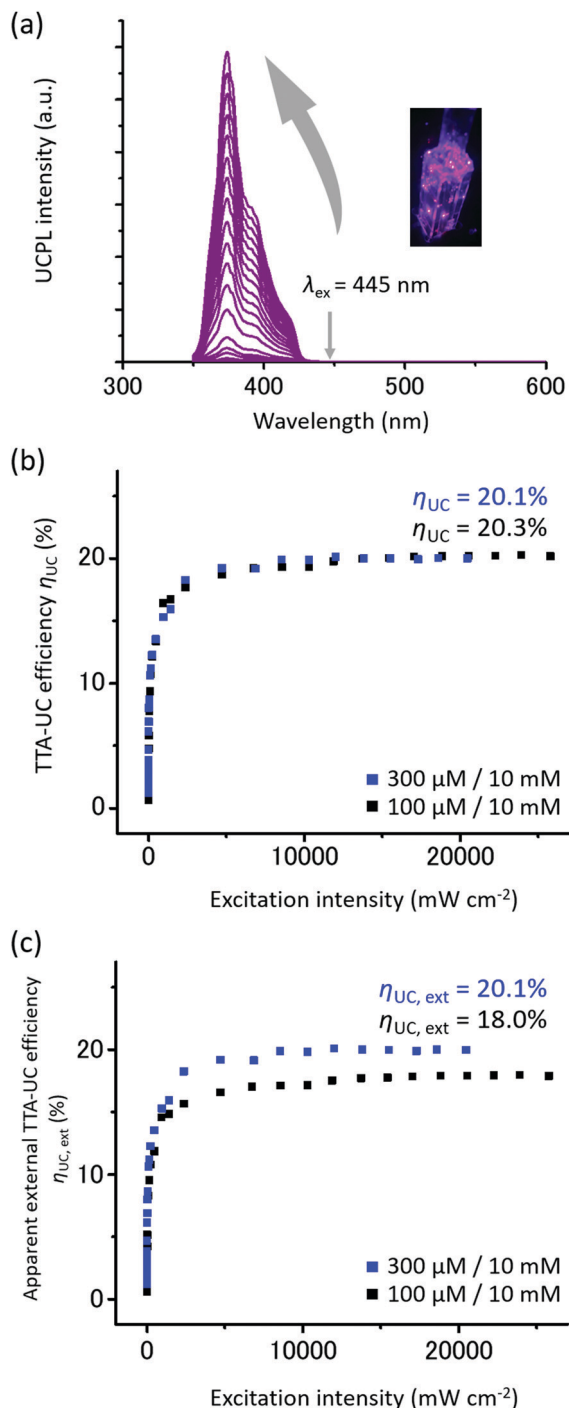


Fig. 3 (a) Upconversion photoluminescence (UCPL) spectra and photograph of the toluene solution of CBDAC (100 μM) and TIPS-Nph (10 mM) ($\lambda_{\text{ex}} = 445 \text{ nm}$, I_{ex} from 1.33 mW cm^{-2} to 25.8 W cm^{-2} , 425 nm short-pass filter). (b) TTA-UC efficiency η_{UC} , and (c) apparent external TTA-UC efficiency $\eta_{\text{UC,ext}}$ of the mixed solution of CBDAC (100 μM (black), 300 μM (blue)) and TIPS-Nph (10 mM) in deaerated toluene.

$\text{Ir}(\text{C}_6)_2(\text{acac})$ and TIPS-Nph showed a TTA-UC efficiency η_{UC} of 21.4% in deaerated toluene (Fig. S6, ESI†). Although CBDAC does not contain any heavy metals, it shows the TTA-UC efficiency comparable to that of the heavy metal-containing

$\text{Ir}(\text{C}_6)_2(\text{acac})$ when combined with TIPS-Nph. This is reasonable considering that the Φ_{ISC} of $\text{Ir}(\text{C}_6)_2(\text{acac})$ has been reported to be nearly 100% and that of CBDAC in benzene has been reported to be as high as 92%.^{28,31} Other parameters that affect the TTA-UC efficiency are expressed as follows,⁴

$$\eta_{\text{UC}} = f\Phi_{\text{ISC}}\Phi_{\text{TET}}\Phi_{\text{TTA}}\Phi_{\text{FL}} \quad (1)$$

where f is the singlet production probability by TTA, and Φ_{TET} and Φ_{TTA} represent the quantum yields of TET and TTA. The Φ_{TET} values were estimated by measuring the donor phosphorescence quantum yield or triplet lifetime (Fig. S7, S8 and Table S1, see the ESI† for details). The Φ_{TET} values of 96.7% and 99.8% were obtained for $\text{Ir}(\text{C}_6)_2(\text{acac})/\text{TIPS-Nph}$ and CBDAC/TIPS-Nph, respectively. Φ_{TTA} values are assumed to be close to 1 since the excitation intensity is in the linear regime as shown later. By increasing the acceptor concentration from 100 μM to 10 mM, Φ_{FL} decreased from 74.8% to 65.5%, which has been reported to be due to the inner-filter effect (Fig. S9, ESI†).²⁸ From these parameters of $\text{Ir}(\text{C}_6)_2(\text{acac})/\text{TIPS-Nph}$, f value of 33.8% was estimated for TIPS-Nph in toluene (Table S1, ESI†), and this value is comparable to that in THF (32%).²⁸ By using this f value and other parameters, the Φ_{ISC} value of CBDAC in toluene was estimated as 91.9%, which is same as the reported value in benzene (92%).³¹ These results indicate that all parameters including Φ_{ISC} and Φ_{TET} are almost the same for $\text{Ir}(\text{C}_6)_2(\text{acac})$ and CBDAC, demonstrating the remarkable potential of CBDAC as the heavy metal-free triplet sensitizer. The triplet lifetime of TIPS-Nph became slightly shorter when the concentration of CBDAC was increased (Fig. S4, ESI†), suggesting the existence of triplet back energy transfer from TIPS-Nph to CBDAC, and further improvement of the TTA-UC efficiency can be expected by tuning the energy levels of donor and acceptor.

Besides the high η_{UC} , the threshold excitation intensity I_{th} is also one of the important parameters in evaluating the performance of TTA-UC.^{42–44} In the typical TTA-UC systems, the UC emission intensity depends on the excitation intensity quadratically in the low intensity region and linearly in the high intensity region. Double logarithmic plots of UC emission intensity of CBDAC and TIPS-Nph against excitation intensity showed a transition from the slope of 2 to 1, and a relatively low I_{th} value of 38.0 mW cm^{-2} was obtained. To further reduce the I_{th} value, we increased the donor concentration from 100 μM to 300 μM , which provided an even lower I_{th} of 10.8 mW cm^{-2} (Fig. S10, ESI†). This value is close to the solar irradiance of 1.4 mW cm^{-2} for $445 \pm 5 \text{ nm}$.

While the UC efficiency η_{UC} is important for evaluating UC properties, high external UC efficiency must be achieved for practical applications. The apparent external UC efficiency $\eta_{\text{UC,ext}}$ is calculated by multiplying the TTA-UC efficiency by the absorption ratio,

$$\eta_{\text{UC,ext}} = \eta_{\text{UC}} \times (1 - 10^{-A}) \quad (2)$$

where A is the absorbance of the donor at the excitation wavelength. Fig. 3c shows the excitation intensity dependence of $\eta_{\text{UC,ext}}$ for CBDAC/TIPS-Nph with different CBDAC

concentrations (100 μM , 300 μM). The high $\eta_{\text{UC,ext}}$ of 18.0% and 20.1% were obtained when the donor concentrations were 100 μM and 300 μM , respectively (Fig. 3c). The reason why η_{UC} and $\eta_{\text{UC,ext}}$ are almost the same for the sample containing 300 μM of CBDAC is probably due to the fact that the inner-filter effect is minimized by monitoring the TTA-UC emission from the direction of the laser-irradiated surface of the sample, in addition to the large absorption ratio of 99.8% and the small reabsorption by CBDAC. The difference in the $\eta_{\text{UC,ext}}$ value between the samples containing 100 and 300 μM of CBDAC is mainly due to the different absorption ratios (88.6% and 99.8%, respectively).

In most systems, due to the large absorption of the donor in the UV region, it is necessary to reduce the concentration of the donor to prevent the decrease in the TTA-UC efficiency η_{UC} by the reabsorption and back energy transfer. Therefore, it has been difficult to obtain a high apparent external UC efficiency due to the small absorbance of the donor. As discussed in our previous report,²⁸ the small absorption of $\text{Ir}(\text{C}_6)_2(\text{acac})$ in the UV region allows us to concomitantly achieve both high visible absorbance and high TTA-UC efficiency η_{UC} at high donor concentration, resulting in a high apparent external UC efficiency $\eta_{\text{UC,ext}}$. Similarly, in the present heavy metal-free system, the high $\eta_{\text{UC,ext}}$ was achieved because CBDAC exhibits strong visible absorption and weak UV absorption, which are notable characteristics of the employed coumarin derivatives.

In conclusion, we showed the highest TTA-UC efficiency η_{UC} of 20.3% as a heavy metal-free vis-to-UV TTA-UC, which is more than double the previous record. This high value was also confirmed by the absolute method. Inspired by the previous high efficiency using $\text{Ir}(\text{C}_6)_2(\text{acac})$,²⁸ we found that CBDAC, the heavy metal-free ketocoumarin derivative, acts as the excellent donor for vis-to-UV TTA-UC. CBDAC exhibits strong visible absorption, weak UV absorption, and high ISC efficiency, which are completely comparable to $\text{Ir}(\text{C}_6)_2(\text{acac})$. Therefore, the heavy metal-free CBDAC/TIPS-Nph system successfully showed high TTA-UC efficiency as well as low I_{th} and high apparent external TTA-UC. This study will provide important guidelines for the future development of heavy metal-free and sustainable UV-generating materials.

Author contributions

N. Y. conceived the project. M. U. and N. H. carried out the experiments and calculations. M. S. and K. M. contributed to the transient absorption measurements. M. U. and N. Y. wrote the manuscript, with the input of N. H., K. O. and N. K.

Conflicts of interest

The authors declare no conflict of interest.

Acknowledgements

This work was partly supported by JSPS KAKENHI (grant numbers JP20H02713, JP20K21211, JP20H05676, JP21J21739),

GAP NEXT program, KYUTEC research and development grant, and the Innovation inspired by Nature Program of Sekisui Chemical Co. Ltd.

References

- 1 S. Balushev, T. Miteva, V. Yakutkin, G. Nelles, A. Yasuda and G. Wegner, *Phys. Rev. Lett.*, 2006, **97**, 143903.
- 2 T. N. Singh-Rachford and F. N. Castellano, *Coord. Chem. Rev.*, 2010, **254**, 2560–2573.
- 3 J. Zhao, S. Ji and H. Guo, *RSC Adv.*, 2011, **1**, 937–950.
- 4 A. Monguzzi, R. Tubino, S. Hoseinkhani, M. Campione and F. Meinardi, *Phys. Chem. Chem. Phys.*, 2012, **14**, 4322–4332.
- 5 Y. C. Simon and C. Weder, *J. Mater. Chem.*, 2012, **22**, 20817–20830.
- 6 S. P. Hill and K. Hanson, *J. Am. Chem. Soc.*, 2017, **139**, 10988–10991.
- 7 V. Gray, K. Moth-Poulsen, B. Albinsson and M. Abrahamsson, *Coord. Chem. Rev.*, 2018, **362**, 54–71.
- 8 B. D. Ravetz, A. B. Pun, E. M. Churchill, D. N. Congreve, T. Rovis and L. M. Campos, *Nature*, 2019, **565**, 343–346.
- 9 S. Wiegand, A. S. Bieber, Z. A. VanOrman, L. Daley, M. Leger, J. P. Correa-Baena and L. Nienhaus, *Matter*, 2019, **1**, 705–719.
- 10 V. Gray, J. R. Allardice, Z. Zhang and A. Rao, *Chem. Phys. Rev.*, 2021, **2**, 031305.
- 11 W. Zhao and F. N. Castellano, *J. Phys. Chem. A*, 2006, **110**, 11440–11445.
- 12 P. Duan, N. Yanai and N. Kimizuka, *Chem. Commun.*, 2014, **50**, 13111–13113.
- 13 X. Jiang, X. Guo, J. Peng, D. Zhao and Y. Ma, *ACS Appl. Mater. Interfaces*, 2016, **8**, 11441–11449.
- 14 V. Gray, P. Xia, Z. Huang, E. Moses, A. Fast, D. A. Fishman, V. I. Vullev, M. Abrahamsson, K. Moth-Poulsen and M. L. Tang, *Chem. Sci.*, 2017, **8**, 5488–5496.
- 15 K. Okumura, N. Yanai and N. Kimizuka, *Chem. Lett.*, 2019, **48**, 1347–1350.
- 16 S. He, X. Luo, X. Liu, Y. Li and K. Wu, *J. Phys. Chem. Lett.*, 2019, **10**, 5036–5040.
- 17 B. Pfund, D. M. Steffen, M. R. Schreier, M. S. Bertrams, C. Ye, K. Börjesson, O. S. Wenger and C. Kerzig, *J. Am. Chem. Soc.*, 2020, **142**, 10468–10476.
- 18 S. Hisamitsu, J. Miyano, K. Okumura, J. K. H. Hui, N. Yanai and N. Kimizuka, *ChemistryOpen*, 2020, **9**, 14–17.
- 19 Y. Kawashima, H. Kouno, K. Orihashi, K. Nishimura, N. Yanai and N. Kimizuka, *Mol. Syst. Des. Eng.*, 2020, **5**, 792–796.
- 20 T. N. Singh-Rachford and F. N. Castellano, *J. Phys. Chem. A*, 2009, **113**, 5912–5917.
- 21 J. Peng, X. Guo, X. Jiang, D. Zhao and Y. Ma, *Chem. Sci.*, 2016, **7**, 1233–1237.
- 22 N. Yanai, M. Kozue, S. Amemori, R. Kabe, C. Adachi and N. Kimizuka, *J. Mater. Chem. C*, 2016, **4**, 6447–6451.
- 23 Q. Chen, Y. Liu, X. Guo, J. Peng, S. Garakyaraghi, C. M. Papa, F. N. Castellano, D. Zhao and Y. Ma, *J. Phys. Chem. A*, 2018, **122**, 6673–6682.

- 24 H. L. Lee, M. S. Lee, H. Park, W. S. Han and J. H. Kim, *Korean J. Chem. Eng.*, 2019, **36**, 1791–1798.
- 25 D. Han, X. Yang, J. Han, J. Zhou, T. Jiao and P. Duan, *Nat. Commun.*, 2020, **11**, 5659.
- 26 Y. Murakami, A. Motooka, R. Enomoto, K. Niimi, A. Kaiho and N. Kiyoyanagi, *Phys. Chem. Chem. Phys.*, 2020, **22**, 27134–27143.
- 27 T. J. B. Zähringer, M. S. Bertrams and C. Kerzig, *J. Mater. Chem. C*, 2022, DOI: 10.1039/d1tc04782e.
- 28 N. Harada, Y. Sasaki, M. Hosoyamada, N. Kimizuka and N. Yanai, *Angew. Chem., Int. Ed.*, 2021, **60**, 142–147.
- 29 L. Hou, A. Olesund, S. Thurakkal, X. Zhang and B. Albinsson, *Adv. Funct. Mater.*, 2021, 2106198.
- 30 D. Huang, J. Sun, L. Ma, C. Zhang and J. Zhao, *Photochem. Photobiol. Sci.*, 2013, **12**, 872–882.
- 31 D. P. Specht, P. A. Martic and S. Farid, *Tetrahedron*, 1982, **38**, 1203–1211.
- 32 J. B. Borak and D. E. Falvey, *Photochem. Photobiol. Sci.*, 2010, **9**, 854–860.
- 33 R. Dong, K. K. Chen, P. Wang, N. Zhang, S. Guo, Z. M. Zhang and T. B. Lu, *Dyes Pigm.*, 2019, **166**, 84–91.
- 34 P. S. Song and K. J. Tapley, Jr., *Photochem. Photobiol.*, 1979, **29**, 1177–1197.
- 35 J. J. Serrano-Pérez, M. Merchán and L. Serrano-Andrés, *Chem. Phys. Lett.*, 2007, **434**, 107–110.
- 36 S. Aloïse, C. Ruckebusch, L. Blanchet, J. Réhault, G. Buntinx and J. P. Huvenne, *J. Phys. Chem. A*, 2008, **112**, 224–231.
- 37 M. Hussain, J. Zhao, W. Yang, F. Zhong, A. Karatay, H. G. Yaglioglu, E. A. Yildiz and M. Hayvali, *J. Lumin.*, 2017, **192**, 211–217.
- 38 M. Koharagi, N. Harada, K. Okumura, J. Miyano, S. Hisamitsu, N. Kimizuka and N. Yanai, *Nanoscale*, 2021, **13**, 19890–19893.
- 39 Y. Zhou, F. N. Castellano, T. W. Schmidt and K. Hanson, *ACS Energy Lett.*, 2020, **5**, 2322–2326.
- 40 J. C. de Mello, H. F. Wittmann and R. H. Friend, *Adv. Mater.*, 1997, **9**, 230–232.
- 41 N. Yanai, K. Suzuki, T. Ogawa, Y. Sasaki, N. Harada and N. Kimizuka, *J. Phys. Chem. A*, 2019, **123**, 10197–10203.
- 42 A. Monguzzi, J. Mezyk, F. Scotognella, R. Tubino and F. Meinardi, *Phys. Rev. B: Condens. Matter Mater. Phys.*, 2008, **78**, 195112.
- 43 Y. Y. Cheng, T. Khoury, R. G. C. R. Clady, M. J. Y. Tayebjee, N. J. Ekins-Daukes, M. J. Crossley and T. W. Schmidt, *Phys. Chem. Chem. Phys.*, 2010, **12**, 66–71.
- 44 A. Haefele, J. Blumhoff, R. S. Khnayzer and F. N. Castellano, *J. Phys. Chem. Lett.*, 2012, **3**, 299–303.